
MoMo: Momentum Models for Adaptive Learning Rates

Fabian Schaipp

Technical University of Munich
 fabian.schaipp@tum.de

Ruben Ohana

Flatiron Institute, CCM
 rohana@flatironinstitute.org

Michael Eickenberg

Flatiron Institute, CCM
 meickenberg@flatironinstitute.org

Aaron Defazio

Meta AI, Fundamental AI Research (FAIR) team
 adefazio@meta.com

Robert M. Gower

Flatiron Institute, CCM
 rgower@flatironinstitute.org

Abstract

We present new adaptive learning rates that can be used with any momentum method. To showcase our new learning rates we develop MoMo and MoMo-Adam, which are SGD with momentum (SGD-M) and Adam together with our new adaptive learning rates. Our MoMo methods are motivated through model-based stochastic optimization, wherein we use momentum estimates of the batch losses and gradients sampled at each iteration to build a model of the loss function. Our model also makes use of any known lower bound of the loss function by using *truncation*. Indeed most losses are bounded below by zero. We then approximately minimize this model at each iteration to compute the next step. For losses with unknown lower bounds, we develop new on-the-fly estimates of the lower bound that we use in our model. Numerical experiments show that our MoMo methods improve over SGD-M and Adam in terms of accuracy *and* robustness to hyperparameter tuning for training image classifiers on MNIST, CIFAR10, CIFAR100, Imagenet32, DLRM on the Criteo dataset, and a transformer model on the translation task IWSLT14.

1 Introduction

Training of a modern production-grade large neural network can cost over 1 million dollars in compute [22]. For instance, the cost for the *Text-to-Text Transfer Transformer* T5-model [18] is estimated to be more than 1.3 million dollars for a single run [22]. What makes training models so expensive is that multiple runs are needed to tune the hyperparameters, with arguably the most important parameter being the learning rate. Indeed, finding a good learning-rate schedule plays a disproportionately large role in the resulting test error of the model, with one extensive study showing that it was at least as important as the choice of optimizer [21].

Here, we develop adaptive learning rates that can be used together with any momentum-based method. To showcase our method, we apply our learning rates to SGD-M (Stochastic Gradient Descent with momentum) and to Adam [7], which gives the MoMo and MoMo-Adam method, respectively. We make use of model-based stochastic optimization [1, 3], and leverage that loss functions are bounded below (typically by zero) to derive our new MoMo (Model-based Momentum) adaptive learning rate.

1.1 The Model-Based Approach

Consider the problem

$$\min_{x \in \mathbb{R}^d} f(x), \quad f(x) := \mathbb{E}_{s \sim \mathcal{D}} [f(x, s)], \quad (1)$$

where $f(x, s)$ is a loss function, s is an input (mini-batch of data), and x are the parameters of a model we are trying to fit to the data. We assume throughout that $f(x, s) \geq 0$, which is the case for most loss functions¹. We also assume that $f(\cdot, s)$ is a continuously differentiable function for all $s \in \mathcal{D}$, that there exists a solution x^* to (1) and denote the optimal value by $f^* := f(x^*) \in \mathbb{R}$.

In our main algorithms MoMo and MoMo-Adam (Algorithms 1 and 2), we present adaptive learning rates² for SGD-M and Adam, respectively. To derive MoMo and MoMo-Adam, we use the model-based viewpoint, which is often motivated by the Stochastic Proximal Point (SPP) [1, 3] method. At each iteration, SPP samples $s_k \sim \mathcal{D}$, then simultaneously minimizes $f(x, s_k)$ while not moving too far from the iterate x^k . Given a step size or learning rate $\alpha_k > 0$, this can be written as

$$x^{k+1} = \operatorname{argmin}_{x \in \mathbb{R}^d} f(x, s_k) + \frac{1}{2\alpha_k} \|x - x^k\|^2. \quad (2)$$

Since this problem needs to be solved at every iteration, it needs to be fast to compute. However, in general (2) is difficult to solve because $f(x, s_k)$ can be a highly nonlinear function. Model-based methods replace $f(x, s_k)$ by a simpler model $m_k(x)$ of the function [1, 3], and update according to

$$x^{k+1} = \operatorname{argmin}_{x \in \mathbb{R}^d} m_k(x) + \frac{1}{2\alpha_k} \|x - x^k\|^2. \quad (3)$$

SGD can be formulated as a model-based method by choosing the model to be the linearization of $f(x, s_k)$ around x^k , that is

$$m_k(x) = f(x^k, s_k) + \langle \nabla f(x^k, s_k), x - x^k \rangle. \quad (4)$$

Using the above $m_k(x)$ in (3) gives the SGD update $x^{k+1} = x^k - \alpha_k \nabla f(x^k, s_k)$, see [1, 19].

Our main insight for developing the MoMo methods is that we should build a model directly for $f(x)$, and not $f(x, s_k)$, since our objective is to minimize $f(x)$. To this end, we develop a model $m_k(x)$ that is a good approximation of $f(x)$ when x is close to x^k , and such that (3) is relatively inexpensive to solve. Our models use only a stream of stochastic samples of the loss and gradient, make use of momentum and leverage the positivity of the loss function.

1.2 Background and Contributions

Momentum and model-based methods. The update formula of many stochastic methods such as SGD can be interpreted by taking a proximal step with respect to a model of the objective function [1, 3]. Independently of this, momentum is incorporated into many methods in order to boost performance.

Contributions. Here we give a new model-based interpretation of momentum, namely that it can be motivated as a model of the objective function $f(x)$ by averaging sampled loss functions. This allows us to naturally combine momentum with other model-based techniques.

Lower bounds and truncated models. One of the main advantages of the model-based viewpoint [1, 3] is that it illustrates how to use knowledge of a lower bound of the function via truncation. Methods using this truncated model are often easier to tune [1, 12, 20].

Contributions. By combining the model-based viewpoint of momentum with a truncated model we arrive at our new MoMo method. Since we are interested in loss functions, we can use zero as a lower bound estimate in many learning tasks. However, for some tasks such as training transformers, the minimal loss is often non-zero. If the non-zero lower bound is known, we can straightforwardly

¹We choose zero as a lower bound for simplicity. Our methods could handle any constant lower bound.

²Here the term *adaptivity* refers to a scalar learning rate that changes from one iteration to the next by using easy-to-compute quantities. This is different from the notion of adaptivity used for Adam or AdaGrad [5], where the learning rate is different for each coordinate. We refer to the latter meaning of adaptivity as *preconditioning*.

incorporate it into our model. For unknown lower bound values we also develop new online estimates of a lower bound in [Section 4](#). Our estimates can be applied to any stochastic momentum-based method, and thus may be of independent interest. Our main influence for this development was D-adaptation [\[4\]](#) which develops an online estimate of the distance to the solution, and uses this to rescale the learning rate.

Adaptive methods. In practice, tuning learning-rate schedules is intricate and computationally expensive. Adam [\[7\]](#) and variants such as AdamW [\[10\]](#), are often easier to tune and are now being used routinely to train DNNs across a variety of tasks. This and the success of Adam have incentivised the development of many new adaptive learning rates, including approaches based on coin-betting [\[13\]](#), variants of AdaGrad [\[4, 5\]](#), and stochastic line search [\[25\]](#).

Contributions. Our new adaptive learning rate can be combined with any momentum based method, and even allows for a preconditioner to be used. For example, Adam is a momentum method that makes use of a preconditioner. By using this viewpoint, together with a lower bound, we derive an extension of Adam which we call MoMo-Adam.

Adaptive Polyak step sizes. For convex, non-smooth optimization, Polyak proposed an adaptive step size using the current objective function value $f(x^k)$ and the optimal value f^* [\[17\]](#). Recently, the Polyak step size has been adapted to the stochastic setting [\[2, 6, 9, 14\]](#). For example, [\[9\]](#) proposed SPS_{\max} given by

$$x^{k+1} = x^k - \min \left\{ \gamma_b, \frac{f(x^k, s_k) - \inf_z f(z, s_k)}{c \|\nabla f(x^k, s_k)\|^2} \right\} \nabla f(x^k, s_k), \quad (\text{SPS}_{\max})$$

where $c, \gamma_b > 0$. The stochastic Polyak step size is closely related to stochastic model-based proximal point methods as well as stochastic bundle methods [\[1, 16, 20\]](#).

Contributions. Our proposed method MoMo can be seen as an extension of the Polyak step size that also incorporates momentum. This follows from the viewpoint of the Polyak step size [\[16, 20\]](#) as a truncated model-based method. In particular MoMo with no momentum is equal to SPS_{\max} .

Numerical findings. We find that MoMo consistently improves the accuracy *and* the sensitivity with respect to hyperparameter choice as compared to SGD-M for standard image classification tasks including MNIST, CIFAR10, CIFAR100 and Imagenet32. The same is true for MoMo-Adam compared to Adam on encoder-decoder transformers on the translation task IWSLT14.

Furthermore, we observe that the adaptive learning rate of MoMo(-Adam) for some tasks automatically performs a warm-up at the beginning of training and a decay in later iterations, two techniques often used in order to improve training [\[23\]](#).

2 Model-Based Momentum Methods

Let us recall the SGD model in [\(4\)](#) which has two issues: First, it approximates a single stochastic function $f(x, s_k)$, as opposed to the full loss $f(x)$. Second, this model can be negative even though our loss function is always positive. Here, we develop a model directly for $f(x)$, and not $f(x, s_k)$, which also takes into account lower bounds on the function value.

2.1 Deriving MoMo

Suppose we have sampled inputs s_1, \dots, s_k and taken k iterations x^1, \dots, x^k . We can use these past samples to build a better model of $f(x)$ by averaging past function evaluations as follows

$$f(x) = \mathbb{E}_{s \sim \mathcal{D}} [f(x, s)] \approx \frac{1}{\rho_k} \sum_{j=1}^k \rho_{j,k} f(x, s_j), \quad (5)$$

where $\rho_{j,k} \geq 0$ and $\rho_k := \sum_{j=1}^k \rho_{j,k}$. Thus, the $\rho_k^{-1} \rho_{j,k}$ are a discrete probability mass function over the previous samples. The issue with [\(5\)](#) is that it is expensive to evaluate $f(x, s_j)$ for $j = 1, \dots, k$, which we would need to do at every iteration. To address this, we approximate each $f(x, s_j)$

by linearizing $f(x, s_j)$ around the point it was last evaluated, i.e. x^j . This leads to the further approximation

$$f(x, s_j) \approx f(x^j, s_j) + \langle \nabla f(x^j, s_j), x - x^j \rangle, \quad \text{for } j = 1, \dots, k. \quad (6)$$

Using (5) and the linear approximations in (6) we can approximate $f(x)$ as follows

$$f(x) \approx \frac{1}{\rho_k} \sum_{j=1}^k \rho_{j,k} (f(x^j, s_j) + \langle \nabla f(x^j, s_j), x - x^j \rangle). \quad (7)$$

Since we know the loss is lower-bounded by zero, we will also impose a lower bound on our model. Though we could use zero as our lower bound, we will use an estimate $f_*^k \geq 0$ of the lower bound to allow for cases where $f(x^*)$ may be far from zero. Imposing a lower bound of f_*^k gives the following model

$$f(x) \approx \max \left\{ \frac{1}{\rho_k} \sum_{j=1}^k \rho_{j,k} (f(x^j, s_j) + \langle \nabla f(x^j, s_j), x - x^j \rangle), f_*^k \right\} =: m_k(x). \quad (8)$$

For overparametrized machine-learning models the minimum value $f(x^*)$ is often close to zero [6, 11]. Thus, choosing $f_*^k = 0$ in every iteration will work well (as we verify later in our experiments). For tasks where $f_*^k = 0$ is too loose of a bound, in [Section 4](#) we develop an online estimate for f_*^k based on available information. Using the model (8), we can now define the proximal update

$$x^{k+1} = \underset{y \in \mathbb{R}^d}{\operatorname{argmin}} m_k(y) + \frac{1}{2\alpha_k} \|y - x^k\|^2. \quad (9)$$

The following Lemma shows that update (9) can be computed in closed form (proof in [Appendix C.1](#)).

Lemma 2.1. Let

$$d_k := \sum_{j=1}^k \rho_{j,k} \nabla f(x^j, s_j), \quad \bar{f}_k := \sum_{j=1}^k \rho_{j,k} f(x^j, s_j), \quad \gamma_k := \sum_{j=1}^k \rho_{j,k} \langle \nabla f(x^j, s_j), x^j \rangle. \quad (10)$$

The closed form solution to (9) is

$$x^{k+1} = x^k - \underbrace{\min \left\{ \frac{\alpha_k}{\rho_k}, \frac{(\bar{f}_k + \langle d_k, x^k \rangle - \gamma_k - \rho_k f_*^k)_+}{\|d_k\|^2} \right\} d_k}_{:= \tau_k}. \quad (11)$$

Finally, it remains to select the averaging coefficients $\rho_{j,k}$. Here we will use an exponentially weighted average that places more weight on recent samples. Aside from working well in practice on countless real-world examples, using an exponentially weighted average can be motivated in the setting of the proximal update (9). The regularization in the proximal step enforces that x^{k+1} will be close to x^k . In particular, any iterate is likely to be closest to the most recent preceding iterate. Since we want the model $m_k(y)$ to be a reasonably accurate approximation of $f(y)$ when y is close to the current iterate, this justifies using averaging weights $\rho_{j,k}$ that put more weight on the recent iterates, i.e. $\rho_{j,k}$ big for j close to k . We give two options for exponentially weighted averaging next.

2.2 The Coefficients $\rho_{j,k}$: To bias or not to bias

We want to choose $\rho_{j,k} \geq 0$ such that we can update \bar{f}_k , d_k and γ_k in (10) on the fly, storing only two scalars and one vector.

Exponentially Weighted Average. Let $\beta \in [0, 1)$. Starting with $\rho_{1,1} = 1$, and for $k \geq 2$ define

$$\rho_{j,k} = \begin{cases} \beta \rho_{j,k-1}, & j \leq k-1, \\ 1 - \beta, & j = k. \end{cases}$$

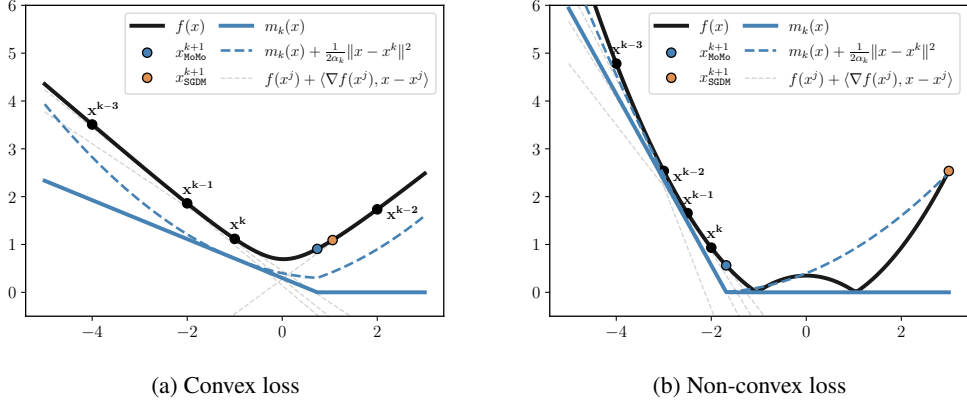


Figure 1: Illustration of the MoMo model (blue curves) for two different loss functions with learning rate $\alpha_k = 5$. Due to truncation, the new iterate of MoMo (blue point) is closer to the minimum than SGD-M (orange point). The right plot shows how MoMo takes a small step when gradients are steep, whereas SGD-M takes a large step and ends up far from the solution as a result.

Then, $\rho_k = \sum_{j=1}^k \rho_{j,k} = 1$ for all $k \in \mathbb{N}$ and the quantities in (10) are exponentially weighted averages. A proof is given in [Lemma A.1](#). As a consequence, we can update \bar{f}_k , d_k and γ_k on the fly as given in lines 4–6 in [Algorithm 1](#). Combining update (11) and the fact that $\rho_k = 1$, we obtain [Algorithm 1](#), which we call MoMo.

Algorithm 1: MoMo: Model-based Momentum method.

1 Default settings: $\alpha_k = 1$ and $\beta = 0.9$
Input: $x^1 \in \mathbb{R}^d$, $\beta \in [0, 1)$,
 $\alpha_k \geq 0$, $(f_*^k)_{k \in \mathbb{N}} \subset \mathbb{R}$
2 Initialize: $\bar{f}_0 = f(x^1, s_1)$, $d_0 = \nabla f(x^1, s_1)$,
 $\gamma_0 = \langle d_0, x^1 \rangle$
3 for $k = 1$ **to** $K - 1$ **do**
4 $\bar{f}_k = (1 - \beta)f(x^k, s_k) + \beta\bar{f}_{k-1}$
5 $\gamma_k = (1 - \beta)\langle \nabla f(x^k, s_k), x^k \rangle + \beta\gamma_{k-1}$
6 $d_k = (1 - \beta)\nabla f(x^k, s_k) + \beta d_{k-1}$
7 $h_k = \bar{f}_k + \langle d_k, x^k \rangle - \gamma_k$
8 $x^{k+1} = x^k - \min \left\{ \alpha_k, \frac{(h_k - f_*^k)_+}{\|d_k\|^2} \right\} d_k$
Output: x^K

Remark 2.2. The *adaptive learning rate* τ_k in (11) determines the size of the step and can vary in each iteration even if α_k is constant. The *(user-specified) learning rate* α_k is used to cap the adaptive learning rate τ_k .

Remark 2.3 (Complexity). MoMo has the same order of iteration complexity and memory footprint as SGD-M. Indeed, MoMo only stores two additional scalars γ_k and \bar{f}_k (h_k can be substituted out) as compared to SGD-M. The additional computational costs are two inner products on lines 5 and 7, and one vector norm on line 8, all of which are $\mathcal{O}(d)$ operations.

For $\beta = 0$ (no momentum), we have $\gamma_k = \langle \nabla f(x^k, s_k), x^k \rangle = \langle d_k, x^k \rangle$ and $\bar{f}_k = f(x^k, s_k)$. Consequently $h_k = f(x^k, s_k)$, and in this special case, MoMo is equivalent³ to [\(SPS_{max}\)](#).

[Fig. 1](#) illustrates how the MoMo model (9) approximates a convex function (left) and a non-convex function (right). We also show how the resulting update x_{MoMo}^{k+1} in [Fig. 1](#) can be closer to minima (left) and sometimes much closer (right) on non-convex problems, as compared to a step of SGD-M.

Averaging with Bias Correction. Choosing $\rho_{j,k} = (1 - \beta)\beta^{k-j}$ for $j = 1, \dots, k$, we have $\rho_{j,k} = \beta\rho_{j,k-1}$, and $\rho_{k,k} = 1 - \beta$. Hence, $\bar{f}_k = (1 - \beta)f(x^k, s_k) + \beta\bar{f}_{k-1}$ and analogously for d_k , γ_k . However, this choice does not satisfy $\sum_{j=1}^k \rho_{j,k} = 1$. Indeed using the geometric series gives

$$\rho_k = (1 - \beta) \sum_{j=0}^{k-1} \beta^j = 1 - \beta^k.$$

³This equivalence requires setting $\gamma_b \leftarrow \alpha_k$, $c \leftarrow 1$, and assuming $f_*^k = \inf_z f(z, s_k)$.

This fact motivates scaling by the factor of $1 - \beta^k$ which was termed *debiasing* in Adam. This alternative averaging scheme leads to a variant of MoMo with bias correction, presented in [Algorithm 5](#) in the Appendix. As the two presented choices of $\rho_{j,k}$ are very similar, we do not expect major differences in their performance (cf. [Remark A.2](#)). However, we will use this averaging scheme in the next section when we derive MoMo-Adam to be consistent with the notation used in Adam.

3 Weight Decay and Preconditioning

In practice, weight decay is widely used in order to improve generalization [26]. Weight decay is related to adding a squared ℓ_2 -regularization to the objective function [8]. We need to carefully adapt our model-based framework in order to include weight decay. Let us consider the case that instead of problem (1) we solve

$$\min_{x \in \mathbb{R}^d} f(x) + \frac{\lambda}{2} \|x\|^2, \quad (12)$$

where $f(x)$ is again the loss function. We build the model m_k for the loss f and keep the ℓ_2 -regularization outside of the model. That is, equation (9) is modified to

$$x^{k+1} = \operatorname{argmin}_{y \in \mathbb{R}^d} m_k(y) + \frac{\lambda}{2} \|y\|^2 + \frac{1}{2\alpha_k} \|y - x^k\|^2. \quad (13)$$

Finally, for the proximal term $\frac{1}{2\alpha_k} \|y - x^k\|^2$ the Euclidean norm may often not be best suited. Many popular methods such as AdaGrad or Adam are based on using a preconditioner for the proximal step. Hence, we allow for an arbitrary norm defined by a symmetric, positive definite matrix $\mathbf{D}_k \in \mathbb{R}^{d \times d}$, i.e. $\|x\|_{\mathbf{D}_k}^2 := \langle \mathbf{D}_k x, x \rangle$. We can now use \mathbf{D}_k to change the metric within our proximal method by updating as follows.

$$x^{k+1} = \operatorname{argmin}_{y \in \mathbb{R}^d} m_k(y) + \frac{1}{2\alpha_k} \|y - x^k\|_{\mathbf{D}_k}^2 + \frac{\lambda}{2} \|y\|_{\mathbf{D}_k}^2. \quad (14)$$

This update (14) still enjoys a closed form solution, as we show next (proof in [Appendix C.2](#)).

Lemma 3.1. The closed form solution to (14) is given by

$$x^{k+1} = \frac{1}{1 + \alpha_k \lambda} \left[x^k - \min \left\{ \frac{\alpha_k}{\rho_k}, \frac{\left((1 + \alpha_k \lambda) (\bar{f}_k - \rho_k f_*^k - \gamma_k) + \langle d_k, x^k \rangle \right)_+}{\|d_k\|_{\mathbf{D}_k^{-1}}^2} \right\} \mathbf{D}_k^{-1} d_k \right] \quad (15)$$

[Lemma 3.1](#) shows how to incorporate weight decay in MoMo: we replace [Line 8](#) in [Algorithm 1](#) by (15) with $\mathbf{D}_k = \mathbf{Id}$ and $\rho_k = 1$. In this case, if $\beta = 0$ (no momentum) then MoMo with weight decay recovers ProxSPS, the proximal version of the stochastic Polyak step size [20].

Deriving MoMo-Adam. Using [Lemma 3.1](#) we can obtain an Adam-version of MoMo by defining \mathbf{D}_k as the diagonal preconditioner of Adam. We introduce the notation $\mathbf{1}_d$ for a d -dimensional vector of ones and $\operatorname{Diag}(v)$ for a diagonal matrix with diagonal entries $v \in \mathbb{R}^d$. Denoting $g_k = \nabla f(x^k, s_k)$, we choose

$$v_k = (1 - \beta_2) v_{k-1} + \beta_2 (g_k \odot g_k), \quad \mathbf{D}_k = \operatorname{Diag}(\epsilon \mathbf{1}_d + \sqrt{v_k / (1 - \beta_2)^k}),$$

where $\beta_2 \in [0, 1]$, $\epsilon > 0$. Here, \odot and $\sqrt{v_k}$ are elementwise multiplication and square-root operations. Using this diagonal preconditioner together with [Lemma 3.1](#) gives [Algorithm 2](#), called MoMo-Adam. Note that here we choose $\rho_{j,k} = (1 - \beta) \beta^{k-j}$ (cf. [Section 2.2](#)) which gives the standard averaging scheme of Adam.

4 Estimating a Lower Bound

So far, we have assumed that lower-bound estimates (f_*^k) are given. However, $f_*^k = 0$ might not always be a tight estimate of f^* (e.g. when training a transformer). In such situations, we derive an

Algorithm 2: MoMo-Adam: Adaptive learning rates for Adam

1 **Default settings:** $\alpha_k = 10^{-2}$, $(\beta_1, \beta_2) = (0.9, 0.999)$, $\epsilon = 10^{-8}$
Input: $x^1 \in \mathbb{R}^d$, $\beta_1, \beta_2 \in [0, 1]$, $\epsilon > 0$, $\alpha_k > 0$, $\lambda \geq 0$, and $(f_*^k)_{k \in \mathbb{N}} \subset \mathbb{R}$.
2 **Initialize:** $\bar{f}_0 = 0$, $d_0 = 0$, $\gamma_0 = 0$, and $v_0 = 0$.
3 **for** $k = 1$ **to** $K - 1$ **do**

4 $g_k = \nabla f(x^k, s_k)$; $d_k = (1 - \beta_1)g_k + \beta_1 d_{k-1}$
5 $v_k = \beta_2 v_{k-1} + (1 - \beta_2)(g_k \odot g_k)$
6 $\mathbf{D}_k = \text{Diag}(\epsilon \mathbf{1}_d + \sqrt{v_k / (1 - \beta_2^k)})$
7 $\bar{f}_k = (1 - \beta_1)f(x^k, s_k) + \beta_1 \bar{f}_{k-1}$
8 $\gamma_k = (1 - \beta_1)\langle g_k, x^k \rangle + \beta_1 \gamma_{k-1}$
9 $\tau_k = \min \left\{ \frac{\alpha_k}{1 - \beta_1^k}, \frac{((1 + \lambda \alpha_k)(\bar{f}_k - \gamma_k - (1 - \beta_1^k)f_*^k) + \langle d_k, x^k \rangle)_+}{\|d_k\|_{\mathbf{D}_k^{-1}}^2} \right\}$
10 $x^{k+1} = \frac{1}{1 + \alpha_k \lambda} [x^k - \tau_k \mathbf{D}_k^{-1} d_k]$

Output: x^K

online estimate of the lower bound. In particular, we will derive a lower bound on

$$\bar{f}_*^k := \frac{1}{\rho_k} \sum_{j=1}^k \rho_{j,k} f(x^*, s_j). \quad (16)$$

This is not the optimal value $f(x^*)$ of our original loss function, but a finite-sample approximation. This is a reasonable approximation since to derive our method we also approximate $f(x)$ in (7) by the analogous weighted sum around x . The following lemma derives an estimate $f_*^k \geq 0$ for (16) by using readily available information for any momentum-based method, such as [Algorithm 2](#).

Lemma 4.1. Let $f(x, s)$ be convex and positive in x for all $s \in \mathcal{D}$. Let $x^* \in \underset{x \in \mathbb{R}^d}{\operatorname{argmin}} f(x)$ and $h_k = \bar{f}_k + \langle d_k, x^k \rangle - \gamma_k$. Let x^k be the iterates generated by (15) with $\lambda = 0$, and let $\eta_k := \prod_{j=2}^k \lambda_{\min}(\mathbf{D}_j^{-1} \mathbf{D}_{j-1})$. It follows that $\bar{f}_*^k \geq f_*^{k+1}$ where

$$f_*^{k+1} := \frac{2 \sum_{j=1}^k \eta_j \tau_j h_j - \|x^1 - x^*\|_{\mathbf{D}_1}^2 - \sum_{j=1}^k \eta_j \tau_j^2 \|d_j\|_{\mathbf{D}_j^{-1}}^2 - 2 \sum_{j=1}^{k-1} \eta_j \tau_j \rho_j \bar{f}_*^j}{2 \eta_k \tau_k \rho_k}. \quad (17)$$

Bootstrapping by using $f_*^k \approx \bar{f}_*^{k-1}$ we have for $k \geq 2$ that

$$f_*^{k+1} = \frac{h_k}{\rho_k} - \frac{\tau_k \|d_k\|_{\mathbf{D}_k^{-1}}^2}{2 \rho_k}. \quad (18)$$

Our estimate f_*^{k+1} is given in (17), and the proof is in [Appendix D.1](#). To simplify the discussion, consider the case without a preconditioner, i.e. $\mathbf{D}_k = \text{Id}$, which leads to $\eta_k = 1$. First, note that f_*^{k+1} depends on $\|x^1 - x^*\|_{\mathbf{D}_1}^2$, which we do not know. Fortunately, $\|x^1 - x^*\|_{\mathbf{D}_1}^2$ does not appear in our recurrence (18), because it only appears in f_*^1 . We can circumvent this initial dependency by simply setting $f_*^1 = 0$.

We need one more precautionary measure, because there is a natural upper bound on our estimator f_*^k that we cannot cross. Consider the general update given in (15). We have to avoid that $\tau_k = 0$, i.e.

$$(1 + \alpha_k \lambda) \rho_k f_*^k \geq (1 + \alpha_k \lambda) (\bar{f}_k - \gamma_k) + \langle d_k, x^k \rangle =: h_k^\lambda. \quad (19)$$

Hence, in each iteration of MoMo or MoMo-Adam, we call the `ResetStar` routine in [Algorithm 3](#) before the update of x^{k+1} that checks if this upper bound has been crossed, and if so, resets f_*^k to be exactly half-way between the upper bound and zero. After updating x^{k+1} we update f_*^{k+1} with `EstimateStar` routine in [Algorithm 4](#), which is an implementation of the recursion in (18). We call the respective methods MoMo* and MoMo-Adam*. For completeness, we give the full algorithm of

MoMo* in [Algorithm 6](#) in the Appendix. We also show for a simple example how the values of f_*^k converge to the true f^* in [Appendix E.2](#).

Algorithm 3: ResetStar	Algorithm 4: EstimateStar
Input: $f_*^k, \alpha_k, \lambda, \rho_k, h_k^\lambda$ 1 if (19) then 2 $f_*^k = \max \left\{ \frac{1}{2} [(1 + \alpha_k \lambda) \rho_k]^{-1} h_k^\lambda, f_*^1 \right\}$ Output: f_*^k	Input: $\bar{f}_k, x^k, \gamma_k, \tau_k, d_k, \mathbf{D}_k, \rho_k$ 1 $h_k = \bar{f}_k + \langle d_k, x_k \rangle - \gamma_k$ 2 $f_*^{k+1} = \max \left\{ \rho_k^{-1} (h_k - \frac{1}{2} \tau_k \ d_k\ _{\mathbf{D}_k^{-1}}^2), f_*^1 \right\}$ Output: f_*^{k+1}

5 Experiments

Here we investigate how using our MoMo adaptive learning rate can improve the stability of both SGD-M and Adam. To do this, for each task and model, we do a comprehensive learning rate sweep for both SGD-M and Adam, and show the resulting validation score for each learning rate. We then do the same with our adaptive variant MoMo and MoMo-Adam and compare the results.

5.1 General Setup

For MoMo and MoMo-Adam, note that the effective step size (cf. [\(15\)](#)) has the form

$$\tau_k = \min \left\{ \frac{\alpha_k}{\rho_k}, \zeta_k \right\}, \quad \zeta_k := \frac{(1 + \alpha_k \lambda) (\bar{f}_k - \rho_k f_*^k - \gamma_k) + \langle d_k, x^k \rangle_+}{\|d_k\|_{\mathbf{D}_k^{-1}}^2}. \quad (20)$$

We refer to [Algorithm 1, Line 8](#) and [Algorithm 2, Line 10](#) for the exact formula for MoMo and MoMo-Adam (in particular, in the above we $\rho_k = 1, \mathbf{D}_k = \mathbf{Id}$ for MoMo). We remark again that we will refer to α_k as the *(user-specified) learning rate* and to τ_k as the *adaptive learning rate/step size*.

5.2 Zero as Lower Bound

First, we compare our MoMo methods to SGD-M and Adam for problems where zero is a reasonably good estimate of the optimal value f^* . For all experiments in this section, we set $f_*^k = 0$ for all $k \in \mathbb{N}$ for MoMo and MoMo-Adam.

Models and Datasets. We do the following classification tasks.

- ResNet110 for CIFAR100,
- ResNet20 and VGG16⁴ for CIFAR10,
- DLRM for Criteo Kaggle Display Advertising Challenge⁵
- MLP for MNIST: two hidden layers of size 100 and ReLU (plots in [Appendix E](#)).

We use batch norm for both ResNet models and VGG16.

Parameter Settings. We use default choices for momentum parameter β for MoMo and SGD-M, and (β_1, β_2) for MoMo-Adam and Adam respectively. The detailed values are listed in [Appendix E, Table 1](#). In the experiments of this section, we do three independently seeded runs (except for DLRM where we use five seeds) and always report averaged values.

Discussion. We investigate the sensitivity of MoMo to the user-specified learning rate. We run MoMo, MoMo-Adam, Adam and SGD-M for a fixed number of epochs (cf. [Table 1](#)) using a constant learning rate $\alpha_k = \alpha_0$.

The plots in [Fig. 2](#) show the accuracy on the validation set, after a fixed number of epochs, of each method when varying the learning rate α_0 . We observe that for small learning rates MoMo behaves

⁴We use the ResNet implementation from https://github.com/akamaster/pytorch_resnet_cifar10/blob/master/resnet.py. We use the VGG16 implementation from <https://github.com/chengyangfu/pytorch-vgg-cifar10/blob/master/vgg.py>.

⁵Dataset from <https://www.kaggle.com/c/criteo-display-ad-challenge>

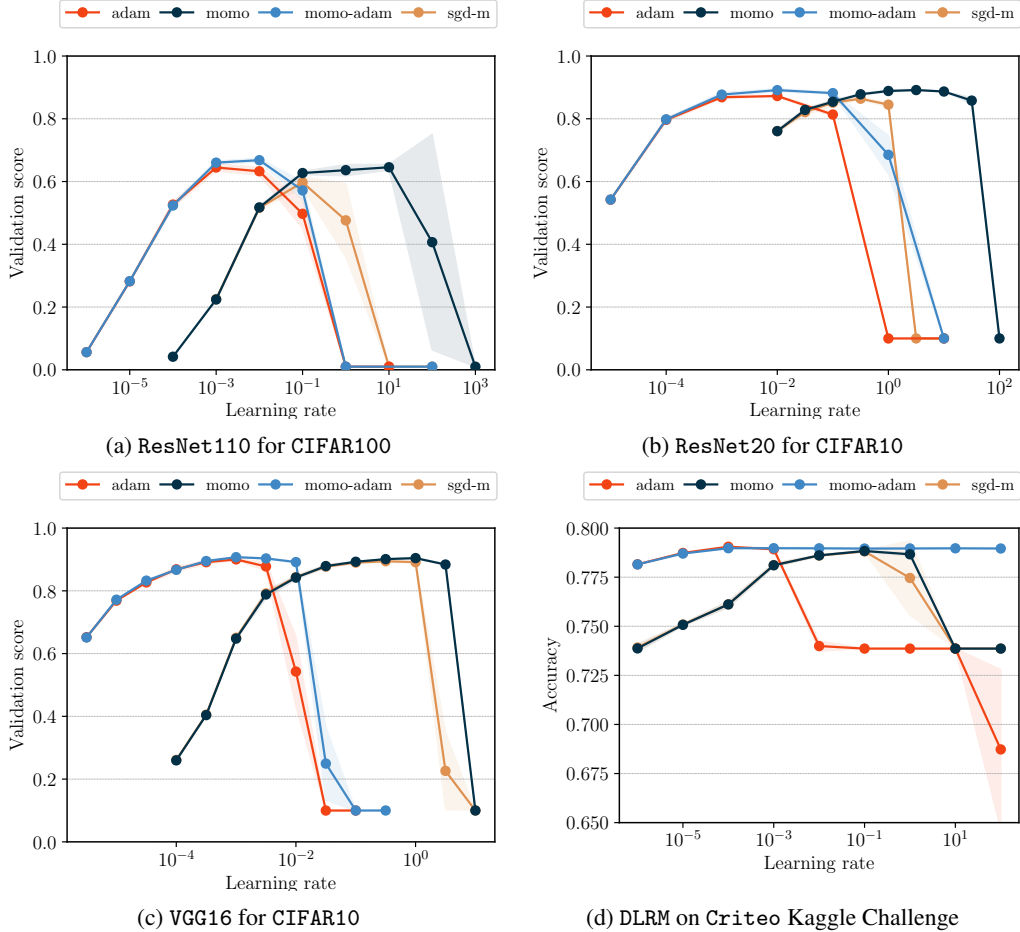


Figure 2: Validation accuracy, after a fixed number of epochs, for varying (constant) learning rate α_0 . Shaded area depicts two standard deviations over three independent runs.

identically to SGD-M. This is expected, since for small α_0 , we have $\tau_k = \alpha_0$ and the update of MoMo is equal to SGD-M. The same applies to the comparison of Adam and MoMo-Adam.

For larger learning rates, we observe that MoMo and MoMo-Adam still work well and in fact improve the accuracy, but SGD-M and Adam decline in performance or even fail to converge. The overall best validation accuracy is achieved by MoMo(-Adam). This advantage can be explained with the adaptivity of the step size of MoMo(-Adam). In Fig. 8a, we plot the adaptive term ζ_k for MoMo for ResNet20. For $\alpha_0 \in [1, 10]$, we have $\tau_k = \zeta_k$ in many iterations, which means that the effective learning rate is adaptive even though α_k is constant. We observe two phenomena: firstly, MoMo is doing an automatic learning rate decay *without any user choice for a learning-rate schedule*. Secondly, in the very first iterations, MoMo is doing a warm-up of the learning rate as $\tau_k = \zeta_k$ starts very small, but quickly becomes large. Both of these dynamics of τ_k help to improve performance and stability. Additionally, we obtain faster initial training progress of MoMo(-Adam) (cf. Fig. 3 and Fig. 6). Our MoMo methods also improve in terms of training loss, plotted in Fig. 7.

For all of the above tasks, the (training) loss converges to values below 0.5. Next, we consider two problems where the final training loss is significantly above zero. In such situations, we find that MoMo methods with $f_*^k = 0$ are less likely to make use of the adaptive term ζ_k for the step size. As a consequence, MoMo with $f_*^k = 0$ will yield little or no improvement and we need to employ the online estimation of a lower bound for MoMo given in Lemma 4.1.

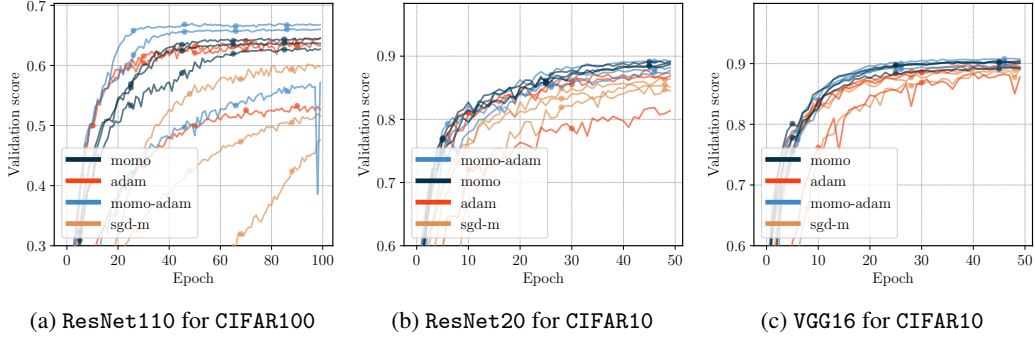


Figure 3: Validation score over training, we plot, for each method, the three choices of α_0 that lead to the best validation score (compare to Fig. 2).

5.3 Online Lower Bound Estimation

We now consider image classification on Imagenet32 and training a transformer for German-to-English translation. For both problems, the optimal value f^* is sufficiently far away from zero and hence we use MoMo with a known estimate of f^* or with the online estimation developed in Section 4. In contrast to the previous experiments, for the following problems we consider as well weight decay and hence use AdamW instead of Adam.

Imagenet32 Classification. We train a ResNet18 for Imagenet32⁶ and give the resulting validation accuracy in Fig. 4. We run two different weight decay values, $\lambda \in \{0, 10^{-4}\}$. We run MoMo(-Adam) first with constant lower bound $f_*^k = 0$ and an *oracle* value $f_*^k = 1.4$. Further, we run MoMo(-Adam)^{*} (indicated by the suffix *-star* in the plots), which correspond to MoMo(-Adam) together with the estimate f_*^k given by Lemma 4.1. See Algorithm 6 for the complete pseudo-code for MoMo^{*}. We compare to SGD-M and AdamW as baseline. For all methods, we use a constant learning rate $\alpha_k = \alpha_0$ and vary the value of α_0 .

First, observe that lower bound $f_*^k = 0$ leads to similar performance as the baseline method (in particular it is never worse). Next, observe that the tighter lower bound $f_*^k = 1.4$ leads to improvement for all learning rates. Finally, we observe that the online estimated lower bound widens the range of sensitivity by an order of magnitude and leads to small improvements in accuracy for $\lambda = 0$.

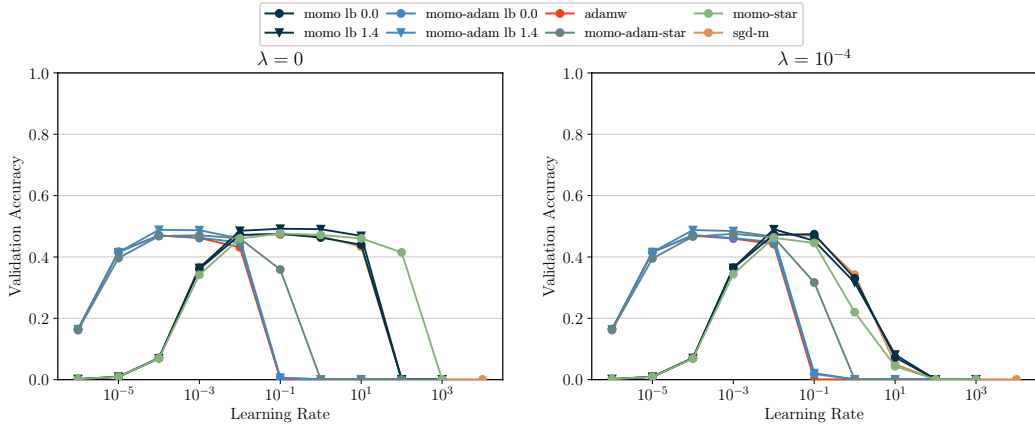


Figure 4: Sensitivity analysis for validation set accuracy on Imagenet32. For two different weight-decay values, $\lambda = 0$ (left) and $\lambda = 10^{-4}$ (right), we plot the validation accuracy as a function of learning rate α_0 for six MoMo methods and two corresponding baselines.

⁶We use the model from <https://github.com/kuangliu/pytorch-cifar/blob/master/models/resnet.py> and only change the last layer size to 1000.

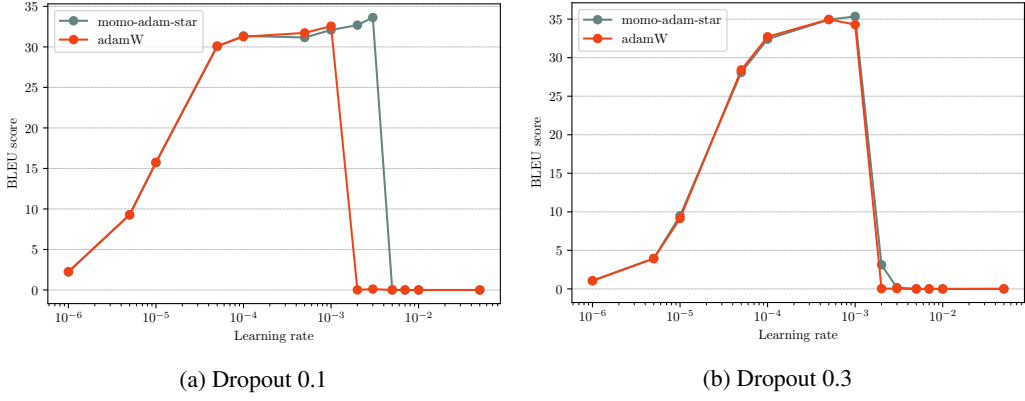


Figure 5: BLEU validation score for the IWSLT14 translation task after training 60 epochs for an encoder-decoder transformer architecture. The x -axis is the initial learning rate α_0 (after warm-up).

Transformer for German-to-English Translation. We consider the task of neural machine translation from German to English by training an encoder-decoder transformer architecture [24] from scratch on the IWSLT14 dataset. We use an architecture from `fairseq` [15] having six encoder and decoder blocks. We consider two settings, namely dropout of 0.1 and 0.3. The training loss is the cross-entropy loss with label smoothing of 0.1. We train for 60 epochs on a NVIDIA A100 80GB.

As a baseline, we run AdamW with fine-tuned hyperparameters: for the learning-rate schedule α_k , we use a linear warm-up of 4000 iterations from zero to a given value α_0 followed by an inverse square-root decay (cf. Fig. 11 for an example curve). We use weight decay of $\lambda = 10^{-4}$, momentum parameters $\beta_1 = 0.9, \beta_2 = 0.98$. The same parameters are also used for MoMo-Adam*. Fig. 5 shows the final BLEU score when varying the initial learning rate α_0 : MoMo-Adam* is on par or better than AdamW on the full range of initial learning rates ranging from 10^{-6} to $5 \cdot 10^{-2}$ and for both dropout values. While the improvement is not as substantial as for previous examples, we remark that here we compare to a heavily fine-tuned configuration of AdamW for this particular task.

6 Conclusion

We present MoMo and MoMo-Adam, adaptive learning rates for SGD-M and Adam. The main conceptual insight is that momentum can be seen as averaging a stream of loss function values and gradients. Combined with truncating this average at a known lower bound of the loss, we obtain the MoMo algorithms. This technique can be applied potentially to other methods, for example variants of Adam.

We show examples where the MoMo methods significantly improve performance of SGD-M and Adam without any tuning of the learning-rate schedule and for a wide range of learning rate values. This can be particularly helpful for practitioners who desire good out-of-the-box optimization performance. We also show how online estimation of the optimal loss value helps to improve the performance of plain MoMo in situations where the optimal loss value is far away from zero. These online estimation techniques are of potential interest to other algorithms and can be further investigated and improved. A further open question for future research is to prove convergence guarantees of the MoMo methods.

References

- [1] Hilal Asi and John C. Duchi. Stochastic (approximate) proximal point methods: convergence, optimality, and adaptivity. *SIAM J. Optim.*, 29(3):2257–2290, 2019.
- [2] Leonard Berrada, Andrew Zisserman, and M. Pawan Kumar. Training neural networks for and by interpolation. In *Proceedings of the 37th International Conference on Machine Learning*, volume 119 of *Proceedings of Machine Learning Research*, pages 799–809. PMLR, 13–18 Jul 2020.
- [3] Damek Davis and Dmitriy Drusvyatskiy. Stochastic model-based minimization of weakly convex functions. *SIAM J. Optim.*, 29(1):207–239, 2019.
- [4] Aaron Defazio and Konstantin Mishchenko. Learning-rate-free learning by D-adaptation, 2023.
- [5] John Duchi, Elad Hazan, and Yoram Singer. Adaptive subgradient methods for online learning and stochastic optimization. *J. Mach. Learn. Res.*, 12:2121–2159, 2011.
- [6] Robert Gower, Othmane Sebbouh, and Nicolas Loizou. SGD for structured nonconvex functions: Learning rates, minibatching and interpolation. In Arindam Banerjee and Kenji Fukumizu, editors, *Proceedings of The 24th International Conference on Artificial Intelligence and Statistics*, volume 130 of *Proceedings of Machine Learning Research*, pages 1315–1323. PMLR, 13–15 Apr 2021.
- [7] Diederik P. Kingma and Jimmy Ba. Adam: A method for stochastic optimization. In Yoshua Bengio and Yann LeCun, editors, *3rd International Conference on Learning Representations, ICLR 2015, San Diego, CA, USA, May 7-9, 2015, Conference Track Proceedings*, 2015.
- [8] Anders Krogh and John Hertz. A simple weight decay can improve generalization. In J. Moody, S. Hanson, and R.P. Lippmann, editors, *Advances in Neural Information Processing Systems*, volume 4. Morgan-Kaufmann, 1991.
- [9] Nicolas Loizou, Sharan Vaswani, Issam Hadj Laradji, and Simon Lacoste-Julien. Stochastic Polyak step-size for SGD: An adaptive learning rate for fast convergence. In Arindam Banerjee and Kenji Fukumizu, editors, *Proceedings of The 24th International Conference on Artificial Intelligence and Statistics*, volume 130 of *Proceedings of Machine Learning Research*, pages 1306–1314. PMLR, 13–15 Apr 2021.
- [10] Ilya Loshchilov and Frank Hutter. Decoupled weight decay regularization. In *7th International Conference on Learning Representations, ICLR 2019, New Orleans, LA, USA, May 6-9, 2019*. OpenReview.net, 2019.
- [11] Siyuan Ma, Raef Bassily, and Mikhail Belkin. The power of interpolation: Understanding the effectiveness of SGD in modern over-parametrized learning. In Jennifer Dy and Andreas Krause, editors, *Proceedings of the 35th International Conference on Machine Learning*, volume 80 of *Proceedings of Machine Learning Research*, pages 3325–3334. PMLR, 10–15 Jul 2018.
- [12] Si Yi Meng, Vasileios Charisopoulos, and Robert M. Gower. A stochastic prox-linear method for CVar minimization. In *OPT 2022: Optimization for Machine Learning (NeurIPS 2022 Workshop)*, 2022.
- [13] Francesco Orabona and Tatiana Tommasi. Training deep networks without learning rates through coin betting. In I. Guyon, U. Von Luxburg, S. Bengio, H. Wallach, R. Fergus, S. Vishwanathan, and R. Garnett, editors, *Advances in Neural Information Processing Systems*, volume 30. Curran Associates, Inc., 2017.
- [14] Antonio Orvieto, Simon Lacoste-Julien, and Nicolas Loizou. Dynamics of SGD with stochastic Polyak stepsizes: Truly adaptive variants and convergence to exact solution. *arXiv*, May 2022.
- [15] Myle Ott, Sergey Edunov, Alexei Baevski, Angela Fan, Sam Gross, Nathan Ng, David Grangier, and Michael Auli. fairseq: A fast, extensible toolkit for sequence modeling. In *Proceedings of NAACL-HLT 2019: Demonstrations*, 2019.
- [16] Alasdair Paren, Leonard Berrada, Rudra P. K. Poudel, and M. Pawan Kumar. A stochastic bundle method for interpolation. *J Mach Learn Res*, 23(15):1–57, 2022.
- [17] Boris T. Polyak. *Introduction to optimization*. Translations Series in Mathematics and Engineering. Optimization Software, Inc., Publications Division, New York, 1987. Translated from the Russian, With a foreword by Dimitri P. Bertsekas.

- [18] Colin Raffel, Noam Shazeer, Adam Roberts, Katherine Lee, Sharan Narang, Michael Matena, Yanqi Zhou, Wei Li, and Peter J. Liu. Exploring the limits of transfer learning with a unified text-to-text transformer. *J Mach Learn Res*, 21(140):1–67, 2020.
- [19] Herbert Robbins and Sutton Monro. A stochastic approximation method. *Ann. Math. Statistics*, 22:400–407, 1951.
- [20] Fabian Schaipp, Robert M. Gower, and Michael Ulbrich. A stochastic proximal Polyak step size. *Transactions on Machine Learning Research*, 2023. Reproducibility Certification.
- [21] Robin M Schmidt, Frank Schneider, and Philipp Hennig. Descending through a crowded valley - benchmarking deep learning optimizers. In Marina Meila and Tong Zhang, editors, *Proceedings of the 38th International Conference on Machine Learning*, volume 139 of *Proceedings of Machine Learning Research*, pages 9367–9376. PMLR, 18–24 Jul 2021.
- [22] Or Sharir, Barak Peleg, and Yoav Shoham. The cost of training nlp models: A concise overview, 2020.
- [23] Ruo-Yu Sun. Optimization for deep learning: An overview. *J. Oper. Res. Soc. China*, 8(2):249–294, jun 2020.
- [24] Ashish Vaswani, Noam Shazeer, Niki Parmar, Jakob Uszkoreit, Llion Jones, Aidan N Gomez, Łukasz Kaiser, and Illia Polosukhin. Attention is all you need. In I. Guyon, U. Von Luxburg, S. Bengio, H. Wallach, R. Fergus, S. Vishwanathan, and R. Garnett, editors, *Advances in Neural Information Processing Systems*, volume 30. Curran Associates, Inc., 2017.
- [25] Sharan Vaswani, Aaron Mishkin, Issam H. Laradji, Mark Schmidt, Gauthier Gidel, and Simon Lacoste-Julien. Painless stochastic gradient: Interpolation, line-search, and convergence rates. In *Advances in Neural Information Processing Systems 32: Annual Conference on Neural Information Processing Systems 2019, NeurIPS 2019, December 8-14, 2019, Vancouver, BC, Canada*, pages 3727–3740, 2019.
- [26] Guodong Zhang, Chaoqi Wang, Bowen Xu, and Roger B. Grosse. Three mechanisms of weight decay regularization. In *7th International Conference on Learning Representations, ICLR 2019, New Orleans, LA, USA, May 6-9, 2019*. OpenReview.net, 2019.
- [27] Zhenxun Zhuang, Mingrui Liu, Ashok Cutkosky, and Francesco Orabona. Understanding AdamW through proximal methods and scale-freeness. *Transactions on Machine Learning Research*, 2022.

Contents

1	Introduction	1
1.1	The Model-Based Approach	2
1.2	Background and Contributions	2
2	Model-Based Momentum Methods	3
2.1	Deriving MoMo	3
2.2	The Coefficients $\rho_{j,k}$: To bias or not to bias	4
3	Weight Decay and Preconditioning	6
4	Estimating a Lower Bound	6
5	Experiments	8
5.1	General Setup	8
5.2	Zero as Lower Bound	8
5.3	Online Lower Bound Estimation	10
6	Conclusion	11
A	Implementation details	15
A.1	Notes on the Averaging Coefficients	15
A.2	Comparison of MoMo-Adam to AdamW	16
A.3	MoMo*	16
B	Auxiliary Lemmas	16
C	Missing Proofs	18
C.1	Proof of Lemma 2.1	18
C.2	Proof of Lemma 3.1	18
D	Estimating a Lower Bound: Proofs and Alternatives	19
D.1	Proof of Lemma 4.1	19
D.2	The Max Lower Bound	21
E	Additional Information on Experiments	22
E.1	Experimental Setup of Section 5.2	22
E.2	Illustrative Example of Online Lower Bound Estimation	22

A Implementation details

A.1 Notes on the Averaging Coefficients

Lemma A.1. Let $\beta \in [0, 1)$. Let $\rho_{1,1} = 1$, and for $k \geq 2$ let

$$\rho_{j,k} = \begin{cases} \beta \rho_{j,k-1}, & j \leq k-1, \\ 1 - \beta, & j = k. \end{cases}$$

Then, $\sum_{j=1}^k \rho_{j,k} = 1$ holds for all $k \in \mathbb{N}$. Further, for an arbitrary sequence $(u_j)_{j \in \mathbb{N}} \subset \mathbb{R}^m$, $m \in \mathbb{N}$, consider the weighted sum

$$\bar{u}_k := \sum_{j=1}^k \rho_{j,k} u_j.$$

Then, if $\bar{u}_0 := u_1$ it holds $\bar{u}_k = (1 - \beta)u_k + \beta\bar{u}_{k-1}$ for all $k \in \mathbb{N}$.

Proof. We prove that $\sum_{j=1}^k \rho_{j,k} = 1$ holds for all $k \in \mathbb{N}$ by induction. For the base case $k = 1$, we have $\rho_{1,1} = 1$ by definition. Assuming that $\sum_{j=1}^{k-1} \rho_{j,k-1} = 1$, we have

$$\sum_{j=1}^k \rho_{j,k} = \rho_{k,k} + \sum_{j=1}^{k-1} \rho_{j,k} = 1 - \beta + \beta \sum_{j=1}^{k-1} \rho_{j,k-1} = 1 - \beta + \beta = 1.$$

Consequently, we have $\bar{u}_1 = \rho_{1,1}u_1 = u_1$, and for $k \geq 2$,

$$\begin{aligned} \bar{u}_k &= \sum_{j=1}^k \rho_{j,k} u_j = (1 - \beta)u_k + \sum_{j=1}^{k-1} \beta \rho_{j,k-1} u_j = (1 - \beta)u_k + \beta \sum_{j=1}^{k-1} \rho_{j,k-1} u_j \\ &= (1 - \beta)u_k + \beta\bar{u}_{k-1}. \end{aligned}$$

□

For the choice of $\rho_{j,k}$ in Lemma A.1, unrolling the recursion, for $k \geq 2$ we obtain the explicit formula

$$\rho_{j,k} = \begin{cases} (1 - \beta)\beta^{k-j}, & j \geq 2 \\ \beta^{k-1}, & j = 1. \end{cases} \quad (21)$$

Averaging with Bias Correction. Below we present a version of MoMo when we use the averaging scheme $\rho_{j,k} = (1 - \beta)\beta^{k-j}$ for $j = 1, \dots, k$.

Algorithm 5: MoMo-Bias: Model-based Momentum with bias correction.

Defaults settings $\beta = 0.9$.

Input: $x^1 \in \mathbb{R}^d$, $\beta \in [0, 1)$, $\alpha_k > 0$, $(f_*^k)_{k \in \mathbb{N}} \subset \mathbb{R}$.
1 Initialize: $\bar{f}_0 = 0$, $d_0 = 0$ and $\gamma_0 = 0$.
2 for $k = 1$ **to** $K - 1$ **do**
3 $\bar{f}_k = (1 - \beta)f(x^k, s_k) + \beta\bar{f}_{k-1}$
4 $d_k = (1 - \beta)\nabla f(x^k, s_k) + \beta d_{k-1}$
5 $\gamma_k = (1 - \beta)\langle \nabla f(x^k, s_k), x^k \rangle + \beta\gamma_{k-1}$
6 $x^{k+1} = x^k - \min \left\{ \frac{\alpha_k}{1 - \beta^k}, \frac{(\bar{f}_k - (1 - \beta^k)f_*^k + \langle d_k, x^k \rangle - \gamma_k)_+}{\|d_k\|^2} \right\} d_k$.
Output: x^K

Remark A.2. [Algorithm 5](#) differs from [Algorithm 1](#) only in two steps: first, the quantities \bar{f}_0 , d_0 , γ_0 are initialized at zero. Secondly, we use $\frac{\alpha_k}{1-\beta^k}$ instead of α_k and $(1-\beta^k)f_*^k$ instead of f_*^k in line (6). As $\beta \in [0, 1)$, for late iteration number k , we can expect that both methods behave very similarly.

A.2 Comparison of MoMo-Adam to AdamW

[Algorithm 2](#) naturally compares to AdamW [10]. Note that the update of AdamW (in the notation of [Algorithm 2](#)) can be written as

$$x^{k+1} = (1 - \alpha_k \lambda) x^k - \frac{\alpha_k}{1 - \beta_1^k} \mathbf{D}_k^{-1} d_k,$$

Compared to [Algorithm 2](#), [Line 10](#), the weight decay of AdamW is not done dividing the whole expression by $\frac{1}{1 + \alpha_k \lambda}$, but instead multiplying only x^k with $1 - \alpha_k \lambda$. This is a first-order Taylor approximation [27]: for α small it holds $\frac{1}{1 + \alpha \lambda} \approx 1 - \alpha \lambda$ and $\frac{\alpha}{1 + \alpha \lambda} \approx \alpha$. If we would want to adapt this approximation, we could replace [Line 10](#) with

$$x^{k+1} = (1 - \lambda \alpha_k) x^k - \min \left\{ \frac{\alpha_k}{1 - \beta_1^k}, \frac{((1 + \lambda \alpha_k)(\bar{f}_k - (1 - \beta_1^k)f_*^k - \gamma_k) + \langle d_k, x^k \rangle)_+}{\|d_k\|_{\mathbf{D}_k^{-1}}^2} \right\} \mathbf{D}_k^{-1} d_k. \quad (22)$$

However, the results of [27] suggest that this approximation has almost no impact on the empirical performance.

A.3 MoMo*

Here we give the complete pseudocode for MoMo*, that is the MoMo method that uses the estimator for f_*^k given in [Lemma 4.1](#).

Algorithm 6: MoMo*: Adaptive learning rates and online estimation of f^* .

Input: $x^1 \in \mathbb{R}^d$, $\beta \in [0, 1)$, $\alpha_k > 0$, $f_*^1 \subset \mathbb{R}$ and sample s_1 .
1 Initialize: $\bar{f}_0 = f(x^1, s_1)$, $d_0 = \nabla f(x^1, s_1)$ and $\gamma_0 = \langle d_0, x^1 \rangle$
2 for $k = 1$ **to** $K - 1$ **do**
 3 $\bar{f}_k = (1 - \beta)f(x^k, s_k) + \beta\bar{f}_{k-1}$
 4 $\gamma_k = (1 - \beta)\langle \nabla f(x^k, s_k), x^k \rangle + \beta\gamma_{k-1}$
 5 $d_k = (1 - \beta)\nabla f(x^k, s_k) + \beta d_{k-1}$
 6 $f_*^k = \text{ResetStar}()$
 7 $x^{k+1} = x^k - \min \left\{ \alpha_k, \frac{(\bar{f}_k - f_*^k + \langle d_k, x^k \rangle - \gamma_k)_+}{\|d_k\|^2} \right\} d_k$
 8 $f_*^{k+1} = \text{EstimateStar}()$.

Output: x^K

B Auxiliary Lemmas

Lemma B.1. Let $y_0, a \in \mathbb{R}^p$ with $a \neq 0$ and $c \in \mathbb{R}$. Let $\beta > 0$. The solution to

$$y^+ = \arg \min_y \underbrace{\left(c + \langle a, y - y_0 \rangle \right)_+}_{:= h(y)} + \frac{1}{2\beta} \|y - y_0\|^2 \quad (23)$$

is given by

$$y^+ = y_0 - \min \left\{ \beta, \underbrace{\frac{(c)_+}{\|a\|^2}}_{:= \tau} \right\} a.$$

Moreover we have $h(y^+) = (c - \tau \|a\|^2)_+$ and

$$h(y^+) = c - \tau \|a\|^2, \quad \text{if } c \geq 0. \quad (24)$$

Proof. Clearly, the objective of (23) is strongly convex and therefore there exists a unique solution. The (necessary and sufficient) first-order optimality condition is given by

$$0 = ta + \beta^{-1}(y^+ - y_0), \quad t \in \partial(\cdot)_+(c + \langle a, y - y_0 \rangle). \quad (25)$$

We distinguish three cases:

(P1) Suppose $c < 0$. Then, y_0 satisfies (25) with $t = 0$ and hence $y^+ = y_0$. In this case $\tau = 0$ and $h(y^+) = 0 = (c)_+$.

(P2) Let $\bar{y} := y_0 - \beta a$ and assume $c + \langle a, \bar{y} - y_0 \rangle > 0 \iff c - \beta \|a\|^2 > 0 \iff \frac{c}{\|a\|^2} > \beta$. Then \bar{y} satisfies (25) with $t = 1$ and hence $y^+ = \bar{y}$. As $\beta > 0$, hence $c > 0$ and $\tau = \beta$. As $h(y^+) = c + \langle a, y^+ - y_0 \rangle = c - \beta \|a\|^2$, equation (24) holds.

(P3) If neither $c < 0$ nor $\frac{c}{\|a\|^2} > \beta$ hold, then it must hold $c + \langle a, y^+ - y_0 \rangle = 0$. Then, the optimality condition is $0 = ta + \beta^{-1}(y^+ - y_0)$ for some $t \in [0, 1]$. Hence, $y^+ = y_0 - t\beta a$ and $c + \langle a, y^+ - y_0 \rangle = c - t\beta \|a\|^2 = 0 \iff t = \frac{c}{\beta \|a\|^2}$. As $c \geq 0$ we have $t \geq 0$ and $\frac{c}{\|a\|^2} \leq \beta$ implies $t \leq 1$. Hence, $\tau = \frac{c}{\|a\|^2}$ and $c - \tau \|a\|^2 = c - c = 0$, so (24) holds.

□

Lemma B.2. Let $y_0, a \in \mathbb{R}^p$ with $a \neq 0$ and $c \in \mathbb{R}$. Let $\mathbf{D} \in \mathbb{R}^{p \times p}$ be a symmetric, positive definite matrix. The solution to

$$y^+ = \underset{y \in \mathbb{R}^p}{\operatorname{argmin}} \underbrace{\left(c + \langle a, y - y_0 \rangle \right)_+}_{:= h(y)} + \frac{1}{2\alpha} \|y - y_0\|_{\mathbf{D}}^2 + \frac{\lambda}{2} \|y\|_{\mathbf{D}}^2 \quad (26)$$

is given by

$$y^+ = \frac{1}{1 + \lambda\alpha} \left[y_0 - \underbrace{\min \left\{ \alpha, \frac{((1 + \lambda\alpha)c - \lambda\alpha \langle a, y_0 \rangle)_+}{\|a\|_{\mathbf{D}^{-1}}^2} \right\} \mathbf{D}^{-1} a}_{=: \tau} \right].$$

Furthermore

$$h(y^+) = \left(c - \frac{\lambda\alpha}{1 + \lambda\alpha} \langle a, y_0 \rangle - \frac{\tau}{1 + \lambda\alpha} \|a\|_{\mathbf{D}^{-1}}^2 \right)_+.$$

Proof. First we complete the squares as follows

$$\begin{aligned} \frac{\lambda}{2} \|y\|_{\mathbf{D}}^2 + \frac{1}{2\alpha} \|y - y_0\|_{\mathbf{D}}^2 &= \frac{1}{2\alpha} \|y\|_{(1 + \lambda\alpha)\mathbf{D}}^2 - \frac{1}{\alpha} \langle y, \mathbf{D}y_0 \rangle + \text{cst.}(y) \\ &= \frac{1}{2\alpha} \|y\|_{(1 + \lambda\alpha)\mathbf{D}}^2 - \frac{1}{\alpha} \langle y, (1 + \lambda\alpha)\mathbf{D} \frac{y_0}{1 + \lambda\alpha} \rangle + \text{cst.}(y) \\ &= \frac{1}{2\alpha} \|y - \frac{1}{1 + \lambda\alpha} y_0\|_{(1 + \lambda\alpha)\mathbf{D}}^2 + \text{cst.}(y), \end{aligned}$$

where $\text{cst.}(y)$ denotes terms that are constant in y . Using the above, (26) is equivalent to

$$\begin{aligned} y^+ &= \underset{y \in \mathbb{R}^p}{\operatorname{argmin}} h(y) + \frac{1}{2\alpha} \|y - \frac{1}{1 + \lambda\alpha} y_0\|_{(1 + \lambda\alpha)\mathbf{D}}^2 \\ &= \underset{y \in \mathbb{R}^p}{\operatorname{argmin}} \left(c + \langle a, y - \frac{1}{1 + \lambda\alpha} y_0 \rangle + \left(\frac{1}{1 + \lambda\alpha} - 1 \right) \langle a, y_0 \rangle \right)_+ + \frac{1}{2\alpha} \|y - \frac{1}{1 + \lambda\alpha} y_0\|_{(1 + \lambda\alpha)\mathbf{D}}^2. \end{aligned}$$

Let $\hat{c} := c + \left(\frac{1}{1+\lambda\alpha} - 1\right) \langle a, y_0 \rangle = c - \frac{\lambda\alpha}{1+\lambda\alpha} \langle a, y_0 \rangle$. With this definition, problem (26) is equivalent to

$$y^+ = \operatorname{argmin}_{y \in \mathbb{R}^p} \left(\hat{c} + \langle a, y - \frac{1}{1+\lambda\alpha} y_0 \rangle \right)_+ + \frac{1}{2\alpha} \|y - \frac{1}{1+\lambda\alpha} y_0\|_{(1+\lambda\alpha)\mathbf{D}}^2.$$

Changing variables with $z^+ = \mathbf{D}^{1/2} y^+$, $z = \mathbf{D}^{1/2} y$, and $z_0 = \mathbf{D}^{1/2} y_0$ gives

$$z^+ = \operatorname{argmin}_{z \in \mathbb{R}^p} \left(\hat{c} + \langle \mathbf{D}^{-1/2} a, z - \frac{1}{1+\lambda\alpha} z_0 \rangle \right)_+ + \frac{(1+\lambda\alpha)}{2\alpha} \|z - \frac{1}{1+\lambda\alpha} z_0\|^2.$$

Applying Lemma B.1 with $y_0 \leftarrow \frac{1}{1+\lambda\alpha} z_0$, $c \leftarrow \hat{c}$, $a \leftarrow \mathbf{D}^{-1/2} a$, $\beta \leftarrow \frac{\alpha}{1+\lambda\alpha}$ gives

$$z^+ = \frac{1}{1+\lambda\alpha} z_0 - \underbrace{\min \left\{ \frac{\alpha}{1+\lambda\alpha}, \frac{(\hat{c})_+}{\|a\|_{\mathbf{D}^{-1}}^2} \right\}}_{:=\tau} \mathbf{D}^{-1/2} a.$$

Changing variables back using $y^+ = \mathbf{D}^{-1/2} z^+$, substituting $\hat{c} = c - \frac{\lambda\alpha}{1+\lambda\alpha} \langle a, y_0 \rangle$ and re-arranging the above gives

$$\begin{aligned} y^+ &= \frac{1}{1+\lambda\alpha} y_0 - \min \left\{ \frac{\alpha}{1+\lambda\alpha}, \frac{(c - \frac{\lambda\alpha}{1+\lambda\alpha} \langle a, y_0 \rangle)_+}{\|a\|_{\mathbf{D}^{-1}}^2} \right\} \mathbf{D}^{-1} a \\ &= \frac{1}{1+\lambda\alpha} \left[y_0 - \min \left\{ \alpha, \frac{((1+\lambda\alpha)c - \lambda\alpha \langle a, y_0 \rangle)_+}{\|a\|_{\mathbf{D}^{-1}}^2} \right\} \mathbf{D}^{-1} a \right]. \end{aligned} \quad (27)$$

□

C Missing Proofs

C.1 Proof of Lemma 2.1

Lemma 2.1. Let

$$d_k := \sum_{j=1}^k \rho_{j,k} \nabla f(x^j, s_j), \quad \bar{f}_k := \sum_{j=1}^k \rho_{j,k} f(x^j, s_j), \quad \gamma_k := \sum_{j=1}^k \rho_{j,k} \langle \nabla f(x^j, s_j), x^j \rangle. \quad (10)$$

The closed form solution to (9) is

$$x^{k+1} = x^k - \underbrace{\min \left\{ \frac{\alpha_k}{\rho_k}, \frac{(\bar{f}_k + \langle d_k, x^k \rangle - \gamma_k - \rho_k f_*^k)_+}{\|d_k\|^2} \right\}}_{:=\tau_k} d_k. \quad (11)$$

Proof. Recall problem (9) given by

$$x^{k+1} = \operatorname{argmin}_{y \in \mathbb{R}^d} m_k(y) + \frac{1}{2\alpha_k} \|y - x^k\|^2.$$

Introducing

$$h_k := \sum_{j=1}^k \rho_{j,k} [f(x^j, s_j) + \langle \nabla f(x^j, s_j), x^k - x^j \rangle] = \bar{f}_k + \langle d_k, x^k \rangle - \gamma_k, \quad (28)$$

we have that

$$m_k(y) = \max \left\{ \rho_k^{-1} (h_k + \langle d_k, y - x^k \rangle), f_*^k \right\} = \left(\rho_k^{-1} (h_k + \langle d_k, y - x^k \rangle) - f_*^k \right)_+ + f_*^k. \quad (29)$$

Using (29), dropping the constant term f_*^k , and multiplying with ρ_k , problem (9) is equivalent to

$$x^{k+1} = \operatorname{argmin}_{y \in \mathbb{R}^d} \left(h_k + \langle d_k, y - x^k \rangle - \rho_k f_*^k \right)_+ + \frac{\rho_k}{2\alpha_k} \|y - x^k\|^2.$$

Applying Lemma B.1 with $\beta \leftarrow \rho_k^{-1} \alpha_k$, $c \leftarrow h_k - \rho_k f_*^k$, $a \leftarrow d_k$ and $y_0 \leftarrow x^k$ gives the result. □

C.2 Proof of Lemma 3.1

Lemma 3.1. The closed form solution to (14) is given by

$$x^{k+1} = \frac{1}{1 + \alpha_k \lambda} \left[x^k - \min \left\{ \frac{\alpha_k}{\rho_k}, \frac{((1 + \alpha_k \lambda)(\bar{f}_k - \rho_k f_*^k - \gamma_k) + \langle d_k, x^k \rangle)_+}{\|d_k\|_{\mathbf{D}_k^{-1}}^2} \right\} \mathbf{D}_k^{-1} d_k \right] \quad (15)$$

$= \tau_k$

Proof. Recall problem (14) given by

$$x^{k+1} = \operatorname{argmin}_{y \in \mathbb{R}^d} m_k(y) + \frac{1}{2\alpha_k} \|y - x^k\|_{\mathbf{D}_k}^2 + \frac{\lambda}{2} \|y\|_{\mathbf{D}_k}^2.$$

We use again (29). Dropping the constant term f_*^k , and multiplying with ρ_k , problem (14) is equivalent to

$$x^{k+1} = \operatorname{argmin}_{y \in \mathbb{R}^d} \left(h_k + \langle d_k, y - x^k \rangle - \rho_k f_*^k \right)_+ + \frac{\rho_k}{2\alpha_k} \|y - x^k\|_{\mathbf{D}_k}^2 + \frac{\rho_k \lambda}{2} \|y\|_{\mathbf{D}_k}^2.$$

Now applying Lemma B.2 with $y_0 \leftarrow x^k$, $a \leftarrow d_k$, $c \leftarrow h_k - \rho_k f_*^k$, $\lambda \leftarrow \rho_k \lambda$, $\alpha \leftarrow \rho_k^{-1} \alpha_k$ and $\mathbf{D} \leftarrow \mathbf{D}_k$, we obtain the result. \square

D Estimating a Lower Bound: Proofs and Alternatives

D.1 Proof of Lemma 4.1

Lemma 4.1. Let $f(x, s)$ be convex and positive in x for all $s \in \mathcal{D}$. Let $x^* \in \operatorname{argmin}_{x \in \mathbb{R}^d} f(x)$ and $h_k = \bar{f}_k + \langle d_k, x^k \rangle - \gamma_k$. Let x^k be the iterates generated by (15) with $\lambda = 0$, and let $\eta_k := \prod_{j=2}^k \lambda_{\min}(\mathbf{D}_j^{-1} \mathbf{D}_{j-1})$. It follows that $\bar{f}_*^k \geq f_*^{k+1}$ where

$$f_*^{k+1} := \frac{2 \sum_{j=1}^k \eta_j \tau_j h_j - \|x^1 - x^*\|_{\mathbf{D}_1}^2 - \sum_{j=1}^k \eta_j \tau_j^2 \|d_j\|_{\mathbf{D}_j^{-1}}^2 - 2 \sum_{j=1}^{k-1} \eta_j \tau_j \rho_j \bar{f}_*^j}{2 \eta_k \tau_k \rho_k}. \quad (17)$$

Bootstrapping by using $f_*^k \approx \bar{f}_*^{k-1}$ we have for $k \geq 2$ that

$$f_*^{k+1} = \frac{h_k}{\rho_k} - \frac{\tau_k \|d_k\|_{\mathbf{D}_k^{-1}}^2}{2 \rho_k}. \quad (18)$$

Proof. Consider the update (15) without weight decay, that is $\lambda = 0$, and switching the index $k \rightarrow j$, which is

$$x^{j+1} = x^j - \tau_j \mathbf{D}_j^{-1} d_j,$$

where τ_j is the step size. Subtracting x^* from both sides, taking norms and expanding the squares we have that

$$\|x^{j+1} - x^*\|_{\mathbf{D}_j}^2 = \|x^j - x^*\|_{\mathbf{D}_j}^2 - 2\tau_j \langle d_j, x^j - x^* \rangle + \tau_j^2 \|d_j\|_{\mathbf{D}_j^{-1}}^2. \quad (30)$$

Now let $\delta_{j+1} := \lambda_{\min}(\mathbf{D}_{j+1}^{-1} \mathbf{D}_j)$ and note that for every vector $v \in \mathbb{R}^d$ we have that

$$\delta_{j+1} \|v\|_{\mathbf{D}_{j+1}}^2 \leq \|v\|_{\mathbf{D}_j}^2. \quad (31)$$

Indeed this follows since

$$\begin{aligned} \|v\|_{\mathbf{D}_j}^2 &= v^\top \mathbf{D}_j v = v^\top \mathbf{D}_{j+1}^{1/2} (\mathbf{D}_{j+1}^{-1/2} \mathbf{D}_j \mathbf{D}_{j+1}^{-1/2}) \mathbf{D}_{j+1}^{1/2} v \\ &\geq \lambda_{\min}(\mathbf{D}_{j+1}^{-1} \mathbf{D}_j) \|v\|_{\mathbf{D}_{j+1}}^2 = \delta_{j+1} \|v\|_{\mathbf{D}_{j+1}}^2. \end{aligned}$$

For simplicity, denote $\nabla f_l = \nabla f(x^l, s_l)$, $f_l = f(x^l, s_l)$. We have that

$$\begin{aligned}
\langle d_j, x^j - x^* \rangle &= \sum_{l=1}^j \rho_{l,j} \langle \nabla f_l, x^j - x^* \rangle \\
&= \sum_{l=1}^j \rho_{l,j} (\langle \nabla f_l, x^j - x^l \rangle + \langle \nabla f_l, x^l - x^* \rangle) \\
&\geq \sum_{l=1}^j \rho_{l,j} (\langle \nabla f_l, x^j - x^l \rangle + f_l - f(x^*, s_l)) \quad (\text{by convexity of } f(\cdot, s)) \\
&= \bar{f}_j + \langle d_j, x^j \rangle - \gamma_j - \sum_{l=1}^j \rho_{l,j} f(x^*, s_l) = h_j - \rho_j \bar{f}_*^j.
\end{aligned} \tag{32}$$

Using (31) together with (32) in (30) gives

$$\begin{aligned}
\delta_{j+1} \|x^{j+1} - x^*\|_{\mathbf{D}_{j+1}}^2 &\leq \|x^{j+1} - x^*\|_{\mathbf{D}_j}^2 \\
&= \|x^j - x^*\|_{\mathbf{D}_j}^2 - 2\tau_j \langle d_j, x^j - x^* \rangle + \tau_j^2 \|d_j\|_{\mathbf{D}_j^{-1}}^2 \\
&\leq \|x^j - x^*\|_{\mathbf{D}_j}^2 - 2\tau_j (h_j - \rho_j \bar{f}_*^j) + \tau_j^2 \|d_j\|_{\mathbf{D}_j^{-1}}^2.
\end{aligned} \tag{33}$$

Now we will perform a weighted telescoping. We will multiply the above by $\eta_j > 0$ such that $\delta_{j+1} \eta_j = \eta_{j+1}$, thus $\eta_j = \eta_1 \prod_{l=2}^j \delta_l$. Thus multiplying through by η_j we have that

$$\eta_{j+1} \|x^{j+1} - x^*\|_{\mathbf{D}_{j+1}}^2 \leq \eta_j \|x^j - x^*\|_{\mathbf{D}_j}^2 - 2\eta_j \tau_j (h_j - \rho_j \bar{f}_*^j) + \eta_j \tau_j^2 \|d_j\|_{\mathbf{D}_j^{-1}}^2.$$

Summing up from $j = 1, \dots, k$ and telescoping we have that

$$\begin{aligned}
0 &\leq \eta_{k+1} \|x^{k+1} - x^*\|_{\mathbf{D}_{k+1}}^2 \\
&\leq \eta_1 \|x^1 - x^*\|_{\mathbf{D}_1}^2 - 2 \sum_{j=1}^k \eta_j \tau_j (h_j - \rho_j \bar{f}_*^j) + \sum_{j=1}^k \eta_j \tau_j^2 \|d_j\|_{\mathbf{D}_j^{-1}}^2.
\end{aligned} \tag{34}$$

Re-arranging the above, choosing $\eta_1 = 1$ and isolating \bar{f}_*^k gives

$$2\eta_k \tau_k \rho_k \bar{f}_*^k \geq 2 \sum_{j=1}^k \eta_j \tau_j h_j - \|x^1 - x^*\|_{\mathbf{D}_1}^2 - \sum_{j=1}^k \eta_j \tau_j^2 \|d_j\|_{\mathbf{D}_j^{-1}}^2 - 2 \sum_{j=1}^{k-1} \eta_j \tau_j \rho_j \bar{f}_*^j.$$

Dividing through by $2\eta_k \tau_k \rho_k$ gives the main result. Finally the recurrence follows since, for $k \geq 2$ we have that

$$\begin{aligned}
f_*^{k+1} &:= \frac{2 \sum_{j=1}^k \eta_j \tau_j h_j - \|x^1 - x^*\|_{\mathbf{D}_1}^2 - \sum_{j=1}^k \eta_j \tau_j^2 \|d_j\|_{\mathbf{D}_j^{-1}}^2 - 2 \sum_{j=1}^{k-1} \eta_j \tau_j \rho_j \bar{f}_*^j}{2\eta_k \tau_k \rho_k} \\
&= \frac{\eta_{k-1} \tau_{k-1} \rho_{k-1}}{\eta_k \tau_k \rho_k} \frac{2 \sum_{j=1}^{k-1} \eta_j \tau_j h_j - \|x^1 - x^*\|_{\mathbf{D}_1}^2 - \sum_{j=1}^{k-1} \eta_j \tau_j^2 \|d_j\|_{\mathbf{D}_j^{-1}}^2 - 2 \sum_{j=1}^{k-2} \eta_j \tau_j \rho_j \bar{f}_*^j}{2\eta_{k-1} \tau_{k-1} \rho_{k-1}} \\
&\quad + \frac{\eta_{k-1} \tau_{k-1} \rho_{k-1}}{\eta_k \tau_k \rho_k} \frac{2\eta_k \tau_k h_k - \eta_k \tau_k^2 \|d_k\|_{\mathbf{D}_k^{-1}}^2 - 2\eta_{k-1} \tau_{k-1} \rho_{k-1} \bar{f}_*^{k-1}}{2\eta_{k-1} \tau_{k-1} \rho_{k-1}} \\
&= \frac{2\eta_{k-1} \tau_{k-1} \rho_{k-1} (f_*^k - \bar{f}_*^{k-1}) - \eta_k \tau_k^2 \|d_k\|_{\mathbf{D}_k^{-1}}^2 + 2\eta_k \tau_k h_k}{2\eta_k \tau_k \rho_k}.
\end{aligned}$$

Now bootstrapping by using $f_*^k \approx \bar{f}_*^{k-1}$ gives the result. \square

D.2 The Max Lower Bound

Here we derive an alternative estimate for the lower bound that does not require bootstrapping, contrary to [Lemma 4.1](#).

Lemma D.1. Let $f(x, s)$ be convex and positive in x for every sample s . Furthermore let $x^* \in \underset{x \in \mathbb{R}^d}{\operatorname{argmin}} f(x)$. Consider x^k are the iterates of (15) with $\lambda = 0$ and let

$$\eta_k := \prod_{j=2}^k \lambda_{\min}(\mathbf{D}_j^{-1} \mathbf{D}_{j-1}), \quad \bar{f}_*^k := \frac{1}{\rho_k} \sum_{j=1}^k \rho_{j,k} f(x^*, s_j), \quad h_k := \bar{f}_k + \langle d_k, x^k \rangle - \gamma_k.$$

It follows that

$$\max_{j=1, \dots, k} \bar{f}_*^j \geq f_*^{k+1} := \frac{2 \sum_{j=1}^k \eta_j \tau_j h_j - \|x^1 - x^*\|^2 - \sum_{j=1}^k \eta_j \tau_j^2 \|d_j\|_{\mathbf{D}_j^{-1}}^2}{2 \sum_{j=1}^k \eta_j \tau_j \rho_j}. \quad (35)$$

Furthermore we have the recurrence

$$f_*^{k+1} = \frac{f_*^k \sum_{j=1}^{k-1} \eta_j \tau_j \rho_j + \eta_k \tau_k \left(h_k - \frac{1}{2} \tau_k \|d_k\|_{\mathbf{D}_k^{-1}}^2 \right)}{\sum_{j=1}^k \eta_j \tau_j \rho_j}. \quad (36)$$

In particular when $\mathbf{D}_k = \mathbf{Id}$ for every k , then we have that $\eta_k = 1$ for all k .

Proof. From the step (34) re-arranging we have that

$$\begin{aligned} 2 \left(\max_{j=1, \dots, k} \bar{f}_*^j \right) \left(\sum_{j=1}^k \eta_j \tau_j \rho_j \right) &\geq 2 \left(\sum_{j=1}^k \eta_j \tau_j \rho_j \right) \bar{f}_*^j \\ &\geq 2 \sum_{j=1}^k \eta_j \tau_j h_j - \|x^1 - x^*\|_{\mathbf{D}_1}^2 - \sum_{j=1}^k \eta_j \tau_j^2 \|d_j\|_{\mathbf{D}_j^{-1}}^2, \end{aligned}$$

if we now assume that $\bar{f}_*^j \approx f(x^*)$ (or upper bounding \bar{f}_*^j by a constant) then by substituting in $f(x^*)$, dividing through by $(\sum_{j=1}^k \eta_j \tau_j \rho_j)$ gives the estimate

$$\max_{j=1, \dots, k} \bar{f}_*^j \geq f_*^{k+1} := \frac{2 \sum_{j=1}^k \eta_j \tau_j h_j - \|x^1 - x^*\|_{\mathbf{D}_1}^2 - \sum_{j=1}^k \eta_j \tau_j^2 \|d_j\|_{\mathbf{D}_j^{-1}}^2}{2 \sum_{j=1}^k \eta_j \tau_j \rho_j}.$$

Finally the recurrence follows since

$$\begin{aligned} f_*^{k+1} &= \frac{2 \sum_{j=1}^k \eta_j \tau_j h_j - \|x^1 - x^*\|_{\mathbf{D}_1}^2 - \sum_{j=1}^k \eta_j \tau_j^2 \|d_j\|_{\mathbf{D}_j^{-1}}^2}{2 \sum_{j=1}^k \eta_j \tau_j \rho_j} \\ &= \frac{\sum_{j=1}^{k-1} \eta_j \tau_j \rho_j}{\sum_{j=1}^k \eta_j \tau_j \rho_j} \frac{2 \sum_{j=1}^{k-1} \eta_j \tau_j h_j - \|x^1 - x^*\|_{\mathbf{D}_1}^2 - \sum_{j=1}^{k-1} \eta_j \tau_j^2 \|d_j\|_{\mathbf{D}_j^{-1}}^2}{2 \sum_{j=1}^{k-1} \eta_j \tau_j \rho_j} \\ &\quad + \frac{2 \eta_k \tau_k h_k - \eta_k \tau_k^2 \|d_k\|_{\mathbf{D}_k^{-1}}^2}{2 \sum_{j=1}^k \eta_j \tau_j \rho_j} \\ &= \frac{f_*^k \sum_{j=1}^{k-1} \eta_j \tau_j \rho_j + \eta_k \tau_k \left(h_k - \frac{1}{2} \tau_k \|d_k\|_{\mathbf{D}_k^{-1}}^2 \right)}{\sum_{j=1}^k \eta_j \tau_j \rho_j}. \end{aligned}$$

□

E Additional Information on Experiments

E.1 Experimental Setup of Section 5.2

The choices for momentum parameter β for MoMo and SGD-M, and (β_1, β_2) for MoMo-Adam and Adam respectively, and weight decay λ are listed in Table 1.

For SGD-M we set the dampening parameter equal to the momentum parameter. Like this, SGD-M does an exponentially-weighted average of past gradients and hence is comparable to MoMo for identical learning rate and momentum. For all other hyperparameters we use the Pytorch default values for Adam and SGD-M (unless explicitly stated otherwise).

Name	λ	Epochs	β (SGD-M, MoMo)	β_1, β_2 (Adam, MoMo-Adam)
ResNet110 for CIFAR100	0	100	0.9	(0.9, 0.999)
ResNet20 for CIFAR10	0	50	0.9	(0.9, 0.999)
VGG16 for CIFAR10	0	50	0.9	(0.9, 0.999)
DLRM for Criteo	0	100	0.9	(0.9, 0.999)
MLP for MNIST	0	10	{0.1, 0.9} (MoMo) 0.9 (SGD-M)	(0.9, 0.999)

Table 1: Hyperparameter setting for the experiments in Section 5.2.

E.2 Illustrative Example of Online Lower Bound Estimation

We show how our online estimation of f_*^k , derived in Section 4 and Lemma 4.1, work for a simple example. Consider a regression problem, with synthetic matrix $A \in \mathbb{R}^{200 \times 10}$ and $b \in \mathbb{R}^{200}$. We solve the problem $\min_{x \in \mathbb{R}^{10}} \sum_{i=1}^{200} \frac{1}{2} \|a_i^\top x - b_i\|^2$, where a_i are the rows of A . The data is generated in a way such that there exists \hat{x} with $b = A\hat{x}$ and hence the optimal value is $f^* = 0$.

We now run MoMo(-Adam) with lower bound estimate $f_*^k = -10$ in all iterations, and MoMo(-Adam)^{*} with initialization $f_*^1 = -10$. Clearly, this is not a tight estimate of the optimal value f^* . From Fig. 10a, we see that online estimation of f_*^k , used in MoMo(-Adam)^{*}, improves stability of the training compared to plain MoMo(-Adam) where a constant value $f_*^k = -10$ is used. From Fig. 10b, we also see that the online values of f_*^k converge to $f^* = 0$.

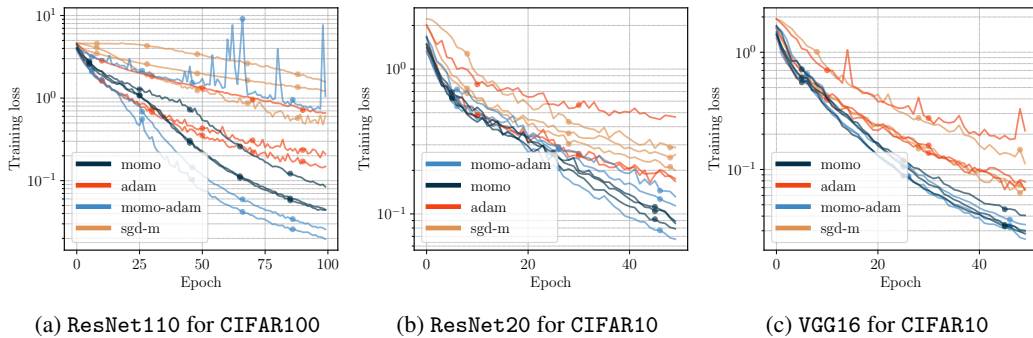


Figure 6: Training loss over training, we plot, for each method, the three choices of α_0 that lead to the best validation score.

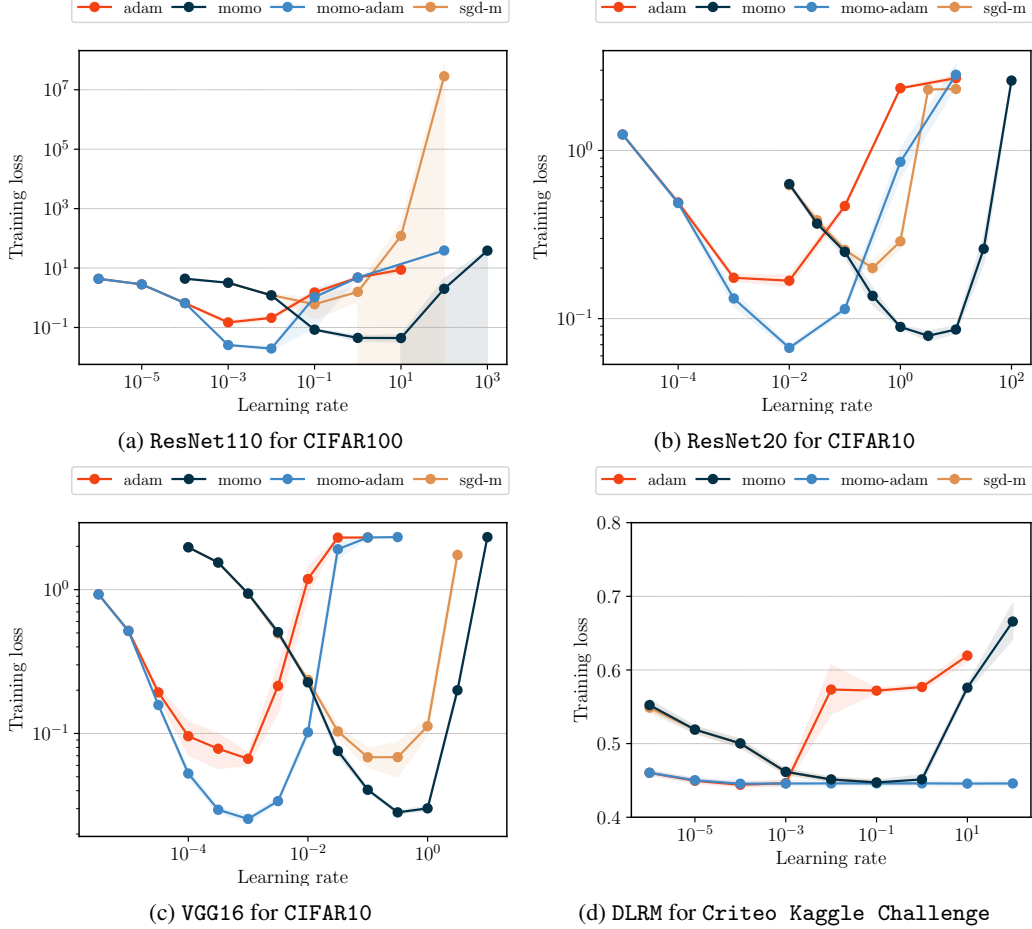


Figure 7: Training loss, after a fixed number of epochs, for varying (constant) learning rate α_0 . Shaded area depicts two standard deviations over three independent runs.

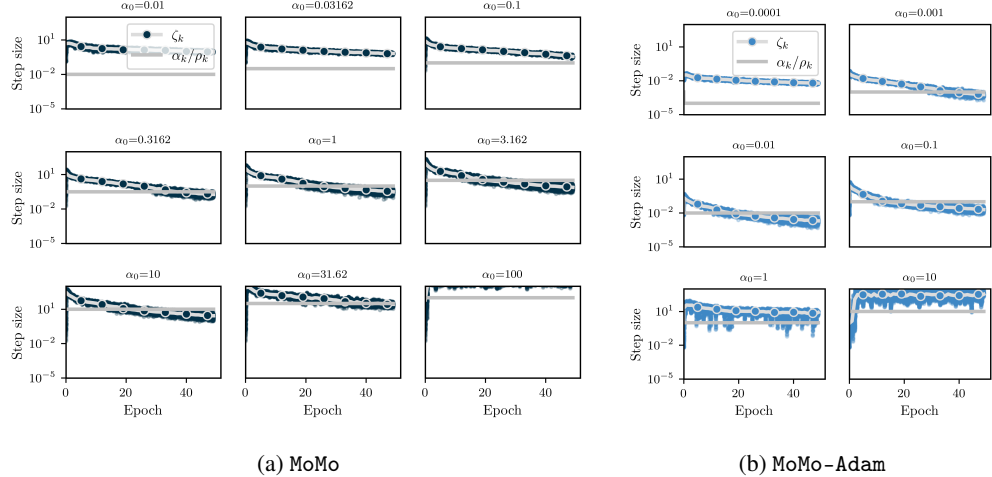


Figure 8: ResNet20 for CIFAR10. Adaptive learning rate of MoMo (left) and MoMo-Adam (right). The colored dots represent the term ζ_k in each iteration. The grey line represents the user-specified learning rate α_k/ρ_k (note that $\rho_k = 1$ for MoMo and $\rho_k \approx 1$ except for the first few iterations in MoMo-Adam). The minimum of the grey line and the dots is the adaptive learning rate $\tau_k = \min\{\frac{\alpha_k}{\rho_k}, \zeta_k\}$ in each iteration. The silver line with colored markers is the median over the values of ζ_k in each epoch.

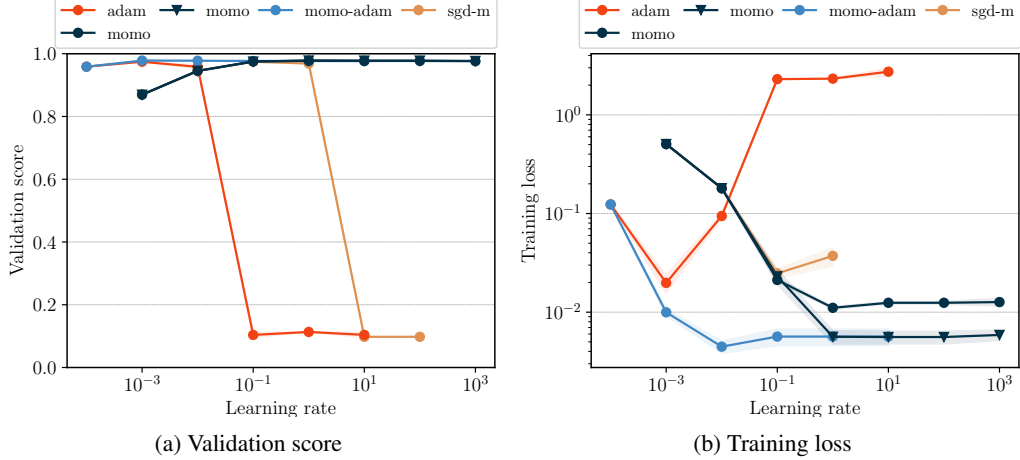


Figure 9: MLP for MNIST. Validation accuracy (left) and training loss (right), after a fixed number of epochs, for varying (constant) learning rate α_0 . Triangle-shaped marker refers to $\beta = 0.9$ and circle-shaped marker to $\beta = 0.1$.

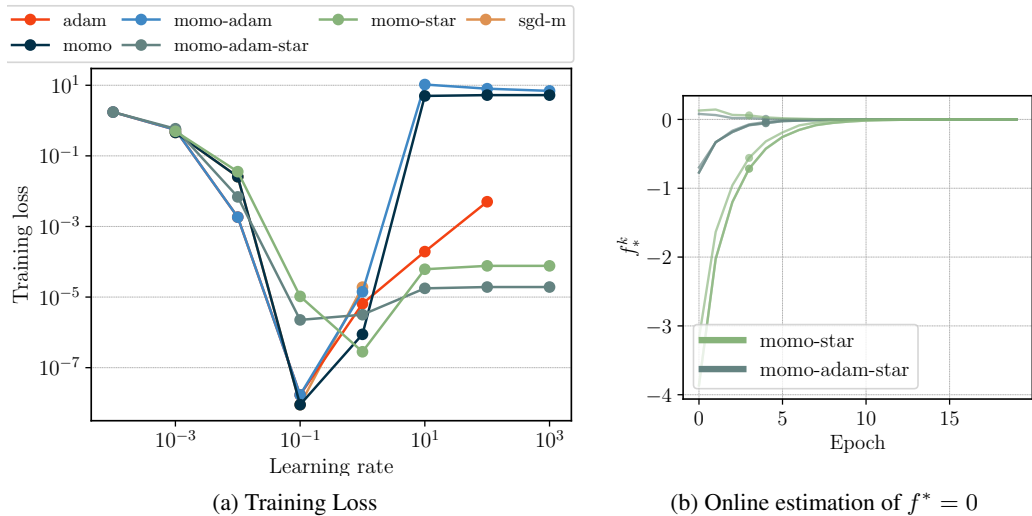


Figure 10: Illustrative example of online lower bound estimation. For all MoMo methods, we initialize $f_*^1 = -10$. Left: Training loss for varying (constant) learning rate α_0 . Right: Value of f_*^k over training, one line corresponds to one choice of α_0 . We plot per method the four values of α_0 that lead to smallest training loss.

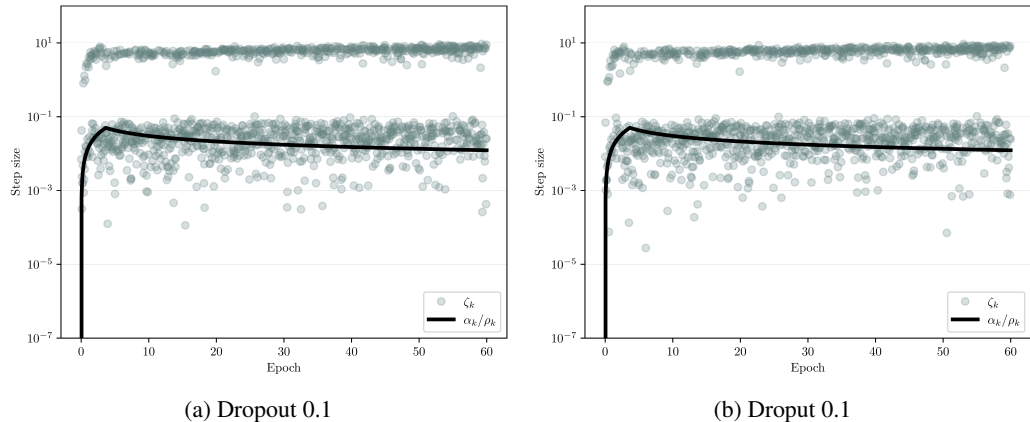


Figure 11: Encoder-decoder transformer for IWSLT14. Adaptive learning rate of MoMo-Adam for $\alpha_0 = 5 \cdot 10^{-2}$. The black line represents the user-specified learning-rate schedule, using linear warm-up followed by an inverse square-root decay.